Bioorganic & Medicinal Chemistry 17 (2009) 6085–6095

Contents lists available at ScienceDirect

Bioorganic & Medicinal Chemistry

journal homepage: www.elsevier.com/locate/bmc

Synthesis, DNA intercalation and 3D QSAR analysis of *cis*-2,4,5-trisubstituted-1,3-dithiolanes as a novel class of antitumor agents

Fei Huang [a], Ming Zhao [b,*], Xiaoyi Zhang [b], Chao Wang [a], Keduo Qian [c], Reen-Yen Kuo [c], Susan Morris-Natschke [c], Kuo-Hsiung Lee [c,*], Shiqi Peng [a,b,*]

[a] College of Pharmaceutical Sciences, Peking University, Beijing 100083, PR China
[b] College of Pharmaceutical Sciences, Capital Medical University, Beijing 100069, PR China
[c] Natural Products Research Laboratories, Eshelman School of Pharmacy, University of North Carolina, Chapel Hill, NC 27599, USA

ARTICLE INFO

Article history:
Received 17 March 2009
Revised 3 June 2009
Accepted 8 June 2009
Available online 13 June 2009

Keywords:
1,3-Dithiolane
Antitumor
DNA-recognition
3D QSAR

ABSTRACT

Acid-catalyzed transacetalation of dimethyl (2*R*,3*S*)-2,3-dimercapto-succinate and 1,1,3,3-tetramethoxypropane provided *cis*-4,5-dimethoxycarbonyl-2-(2′,2′-dimethoxyethyl)-1,3-dithiolane (**2**) in 77% yield. The esterification of **2** and L-amino acids provided 18 active antitumor *cis*-2-carbonylmethyl-4,5- di(L-aminoacyloxymethyl)-1,3-dithiolane analogs (**5a–r**). Five compounds (**5b,c,e,k,p**) exhibited remarkable antitumor activity in in vivo assays. The in vivo antitumor potency of **5e,k,p** at 44.64 μmol/kg was similar to that of cytarabine at 89.28 μmol/kg. Several different assay systems, including UV–vis of CT DNA with or without the representative compound **5d** and CD spectra of CT DNA with or without representative compounds **5b,f,i** demonstrated that DNA is the target of **5a–r**. A 3D QSAR model was established to elucidate quantitative relationships between in vivo antitumor activity and analog structures. An equation with r^2 equal to 0.992 was built to predict antitumor activity of unknown *cis*-2,4,5-trisubstituted-1,3-dithiolane analogs.

1. Introduction

Although several chemotherapeutic drugs including platinum agents, groove binders, alkylating and intercalating agents are routinely used in the clinic for treating cancers, their use still suffers from toxicity and intrinsic or acquired drug resistance. Thus, the discovery of new compounds with potent antitumor activity is still one of the most important goals in medicinal chemistry. Over the past several decades, numerous studies have focused on the design of DNA recognizing molecules. The interaction of a small molecule with DNA initially causes conformational changes in the double helix of DNA, subsequently interrupts replication, transcription, and repair, and finally kills the fast growing cells.[1–3] In the design of small molecules with DNA recognizing capacity, various structures such as harmine and its derivatives,[4–8] anthracyclines,[9] chromium(III) complexes,[10] ellagic acids,[11] neutral red,[12] platinum compounds,[13,14] MLN944,[15] a naphthoquinone,[16] mithramycin,[17] and flavonoids[18] have attracted much interest. Structures containing sulfur have also been explored as antitumor molecules. Some examples are 1,3-dithiane rings, which greatly influenced in vivo effects of some antitumor compounds,[19–21] a dithiazolidinone moiety, which influenced the activity of some small molecules with DNA recognizing capacity,[22,23] and dimethylaminosulfonates of alkane diols or alkenyl thiosulfates, which themselves showed antitumor efficacy.[24,25] The structures of these moieties and compounds are shown in Figure 1. In the present study, we prepared a class of novel 2,4,5-trisubstituted-1,3-dithiolanes and found that they interact with DNA to exhibit antitumor activity. We also analyzed 3D QSAR for the new compounds.

2. Results and discussion

2.1. Synthesis of *cis*-2,4,5-trisubstituted-1,3-dithiolanes

As depicted in Scheme 1, acid-catalyzed transacetalation of dimethyl (2*R*,3*S*)-2,3-dimercaptosuccinate (**1**) and 1,1,3,3-tetrameth-

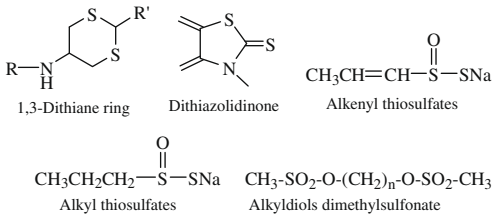

Figure 1. Structures of active antitumor moieties and compounds containing sulfur.

* Corresponding authors. Tel./fax: +86 10 83911528 (S.P.); tel./fax: +86 10 82802482 (M.Z.); tel.: +1 919 962 0066; fax: +1 919 966 3893 (K.-H.L).
E-mail addresses: khlee@unc.edu (K.-H. Lee), sqpeng@email.bjmu.edu.cn (S. Peng).

0968-0896/$ - see front matter © 2009 Elsevier Ltd. All rights reserved.
doi:10.1016/j.bmc.2009.06.011

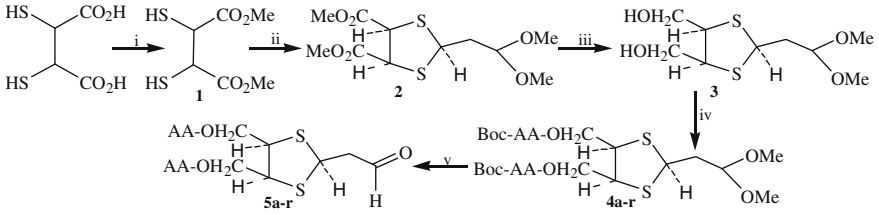

Scheme 1. Synthetic route to *cis*-2,4,5-trisubstituted-1,3-dithiolanes, (i) HCl in MeOH (4 N); (ii) concd HCl, $CHCl_3$, 40 °C or $BF_3{\cdot}Et_2O$, CH_2Cl_2, 0 °C; (iii) $LiAlH_4$/THF, 40 °C; (iv) DMAP/DCC/CH_2Cl_2, room temperature; (v) HCl in EtOAc, 0 °C; In **4a** and **5a** AA = Ala, in **4b** AA = N^G,N^G-$(Boc)_2$-Arg, in **5b** AA = Arg, in **4c** and **5c** AA = Asn, in **4d** and **5d** AA = Gln, in **4e** and **5e** AA = Gly, in **4f** AA = imidazole-*N*-Boc-His, in **5f** AA = His, in **4g** and **5g** AA = Ile, in **4h** and **5h** AA = Leu, in **4i** AA = N^{ω}-Boc-Lys, in **5i** AA = Lys, in **4j** and **5j** AA = Met, in **4k** and **5k** AA = Phe, in **4l** and **5l** AA = Pro, in **4m** and **5m** AA = Ser, in **4n** and **5n** AA = Thr, in **4o** and **5o** AA = Val, in **4p** AA = O-Boc-Tyr, in **5p** AA = Tyr, in **4q** and **5q** AA = Glu(O^tBu), in **4r** and **5r** AA = Trp.

oxypropane provided *cis*-4,5-dimethoxycarbonyl-2-(2′,2′-dimethoxyethyl)-1,3-dithiolane (**2**). The specific catalyst, solvent, and temperature significantly affected the yield of **2**. With concentrated HCl as the catalyst and $CHCl_3$ as the solvent at 40 °C for 48 h, the yield of **2** was 77%. When the reaction was carried out at 25 °C or 0 °C for 48 h, the product was obtained in low yield. With $BF_3{\cdot}Et_2O$ as the catalyst and CH_2Cl_2 as the solvent at 25 °C or 0 °C for 10 min, the yields of **2** were 33% and 75%, respectively. However, with diethyl ether or THF instead of CH_2Cl_2 for 6 h, the reaction provided no desirable product. The data are listed in Table 1. To assign the configuration of **2**, a NOE difference experiment was performed. Positive NOE signals were observed between the methoxy groups at the 2-, 4- and 5-positions. The reported literature values for the coupling constants of ring protons, H-2 and H-5, and CH_2 of 2-dimethoxyethyl of cis-1,3-dioxanes were 9.5, 6.3 and 7.9 Hz, respectively, while those for ring protons, H-2 and H-5, and CH_2 of 2-dimethoxyethyl of *trans*-1,3-dioxanes were 3.9, 7.8 and 3.0–5.3 Hz, respectively.[26,27] Here we found that the coupling constant of ring protons, H-2 and H-4, and CH_2 of 2-dimethoxyethyl of **2** were 7.0, 8.0 and 7.0 Hz, respectively. Based on the results of NOE difference experiment and comparison of the coupling constants of the corresponding protons, we assigned a *cis*-configuration to **2**. Compounds **3**, **4a–r** and **5a–r**, which were derived from **2**, were also assigned as having *cis*-configurations.

Compound **2** was reduced with $LiAlH_4$ in anhydrous THF to give *cis*-4,5-dihydroxymethyl-2-(2′,2′-dimethoxyethyl)-1,3-dithiolane (**3**) in 80% yield. Esterification of **3** with Boc-L-amino acids, promoted by a catalytic amount of DMAP, gave *cis*-4,5-di(*N*-Boc-L-aminoacyloxymethyl)-2-(2′,2′-dimethoxyethyl)-1,3-dithio- lanes (**4a–r**) in yields ranging from 16% to 94%. Removal of the Boc and dimethyl acetal protecting groups by using HCl in EtOAc gave the target *cis*-2-carbonylethyl-4,5-di(L-aminoacyloxymethyl)-1,3-dithiolanes (**5a–r**) in yields ranging from 89% to 98%.

2.2. Antitumor activity of 5a–r

We evaluated in vivo antitumor activity of **5a–r** by using S180 mice as the animal model. Tumor weight was used to correlate the activity of the compounds. The dose-dependent in vivo antitumor effects of **5e**,**k**,**p** were also evaluated.

2.2.1. In vivo antitumor activity of 5a–r

The in vivo assay was carried out according to standard procedures. In the experiments, the tumor weights of S180 mice were used to express the activities of **5a–r** (44.64 μmol/kg/day in 0.2 ml of NS), with 0.2 mL of NS as the negative control and cytarabine (89.28 μmol/kg/day in 0.2 mL of NS) as the positive control. The treatment was carried out for seven consecutive days. The tumor weights of mice receiving **5a–r** are listed in Table 2, while the inhibition percents of the tumor growth are shown with Figure 2. The tumor weights of mice receiving **5a–r** ranged from 0.529 g to 1.493 g. Among the tested compounds, the tumor weights of mice treated with **5b,c,e,k,p** were significantly lower than that of NS-receiving mice (1.240 g, $p < 0.05$–0.01). In addition, the antitumor potency of **5e**,**k**,**p** at 44.64 μmol/kg/day was substantially equal to that of cytarabine (0.582 g, $p > 0.05$) at 89.28 μmol/kg/day. Thus, the data confirmed that the designed 2,4,5-trisubstituted-1,3-dithiolane analogs possess antitumor ability.

Table 1
Effect of reaction condition on the transacetalation

Catalyst	Solvent	Temp. (°C)	Time	Yield (%)
HCl (concentrated)	$CHCl_3$	0	48 h	15
		25	48 h	30
		40	48 h	77
$BF_3{\cdot}Et_2O$	CH_2Cl_2	0	10 min	75
		25	10 min	33
	Ether	0	6 h	0
		25	6 h	0
	THF	0	6 h	0
		25	6 h	0

Table 2
Effect of **5a–r** on tumor growth of S180 mice

Compd[a]	Tumor weight
NS	1.240 ± 0.448
5a	1.213 ± 0.884
5b	0.778 ± 0.265[c]
5c	0.855 ± 0.371[b]
5d	1.061 ± 0.400
5e	0.723 ± 0.203[d]
5f	1.076 ± 0.462
5g	1.064 ± 0.351
5h	1.296 ± 0.596
5i	0.989 ± 0.409
5j	1.139 ± 0.300
Cytarabine	0.582 ± 0.250[c]
5k	0.693 ± 0.248[e]
5l	1.446 ± 0.757
5m	1.493 ± 0.926
5n	1.087 ± 0.400
5o	1.114 ± 0.470
5p	0.529 ± 0.173[e]
5q	1.051 ± 0.608
5r	0.954 ± 0.339
4	1.206 ± 0.414

[a] Tumor weight is expressed by $\overline{X} \pm$ SD g; inhibition is expressed by $\overline{X} \pm$ SD%; NS (normal saline) = vehicle; $n = 10$; **5a–r**: dose = 44.64 μmol/kg; cytarabine: dose = 89.28 μmol/kg.
[b] Compared to NS $p < 0.05$.
[c] Compared to NS $p < 0.01$.
[d] Compared to NS $p < 0.01$, to cytarabine $p > 0.05$.
[e] Compared to NS $p < 0.01$, to cytarabine $p > 0.05$.

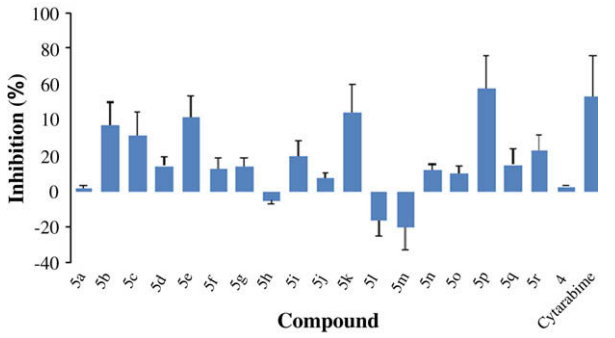

Figure 2. Inhibition percentage of the tumor growth of **5a**–**r** treated mice.

2.2.2. Dose-dependent in vivo antitumor action of 5e,k,p

Compounds with the highest in vivo antitumor activity, namely **5e**,**k**,**p**, were also evaluated for dose-dependent action. Potency increased sequentially for **5e**,**k**,**p** at 0.45, 4.46, and 44.64 μmol/kg. Therefore, compounds **5e,k,p** exhibited dose-dependent anticancer action (Fig. 3).

2.3. Spectral evidence for interaction of 5a–r with DNA

DNA spectra are widely used to study the interactions of small molecules with DNA. To reveal the interactions of **5a–r** with DNA in our studies, CT DNA was selected as the model molecule of DNA, and interaction experiments of **5a–r** toward CT DNA were performed, with which the interactions of **5a–r** toward DNA were explored. For some important experiments, for example, UV–vis and CD, tests of this simulation system were performed. The results demonstrated that these experiments not only provide important spectroscopic evidence for the interaction of **5a–r** toward CT DNA, but also prove that this simulation system should be generally useful to define the interaction of *cis*-2,4,5-trisubstituted-1,3-dithiolanes toward DNA.

2.3.1. UV–vis spectra of CT DNA and 5a–r show induced hyperchromic effect

In the UV–vis experiments, spectra of solutions of CT DNA in PBS (pH 7.4, final concentration 10 μM) were recorded. To 2.5 mL of this solution, sequential aliquots (10 μL of each aliquot) of 10 mM **5a–r**, which was transparent in the UV region of 200–360 nm, in PBS (pH 7.4) were added (final concentration ranging from 4 to 40 μM), and the spectra were recorded. Addition of **5a–r** induced a general hyperchromic effect. As a representative example, the UV titration spectra of CT DNA with **5d** are shown in Figure 4. Clearly, addition of **5d** enhanced the intensity of CT DNA. In addition, a bathochromic shift of 8 nm also occurred in the CT DNA spectra.

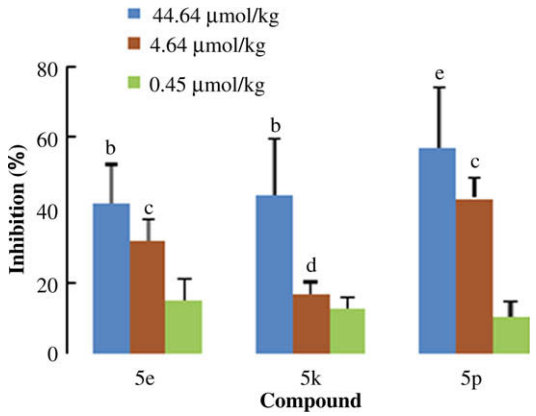

Figure 3. Dose-dependent action of **5e**,**k**,**p** (a) inhibition is expressed by $\bar{X} \pm SD\%$; $n = 10$; (b) compared to 4.46 μmol/kg group $p < 0.01$; (c) compared to 0.45 μmol/kg group $p < 0.01$; (d) compared to 0.45 μmol/kg group $p < 0.05$; (e) compared to 4.46 μmol/kg group $p < 0.05$.

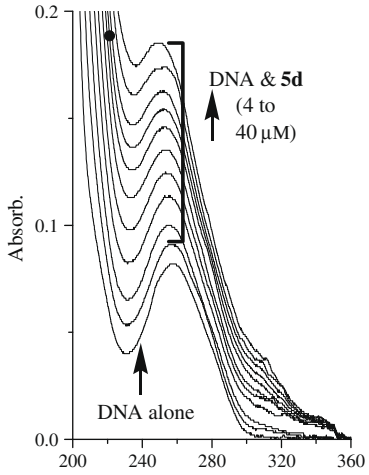

Figure 4. UV titration spectra of 10 μM solution of CT DNA in PBS buffer with 10 mM solution of **5d** in PBS buffer (final concentration 4×10^{-6}, 8×10^{-6}, 1.2×10^{-5}, 1.6×10^{-5}, 2.0×10^{-5}, 2.4×10^{-5}, 2.8×10^{-5}, 3.2×10^{-5} and 4.0×10^{-5} M; pH 7.4).

2.3.2. Effect of 5a–r on the CD spectra of CT DNA

According to general understanding, the circular dichroic (CD) spectrum of CT DNA is characterized by positive and negative bands, of which the former is due to base stacking and the latter is due to right-handed helicity. Interactions of small molecules with CT DNA usually result in intensity changes of the two bands.[28,29] To observe the effects of **5a–r** on the CD spectrum of CT DNA, tests were performed over 200–750 nm. Two mixed solutions (**5a–r** excess solution and **5a–r** stoichiometric solution) of CT DNA and **5a–r** in PBS buffer (pH 7.4) were prepared. The CD spectra of both solutions showed significant intensity decreases in the positive bands and intensity increases in the negative bands. Representative CD spectra of CT DNA alone and CT DNA with **5b,f,i** over 200–300 nm are shown in Figure 5. It was clear that the CT DNA spectra were greatly influenced by addition of **5b,f,i**. These changes in the spectra of CT DNA most likely are results of interactions of CT DNA and **5a–r**.

2.4. 3D QSAR analysis of the in vivo activity of 5a–r

To gain insight into the correlation between the antitumor activity and the structures of **5a–r**, the tumor inhibition of S180 mice receiving **5a–r** were selected as the activity parameter for 3D QSAR analysis. As described below, the equation ($r^2 = 0.992$) that was generated by using the Cerius^2 QSAR module following standard procedures demonstrated that the tumor inhibition of **5a–r** correlated quantitatively with structure. This equation should be capable of predicting the in vivo antitumor activity of unknown *cis*-2,4,5- trisubstituted-1,3-dithiolanes.

2.4.1. Alignment of 5a–r

To establish valid 3D-QSAR models, a proper alignment procedure for **5a–r** was determined using the target model align strategy in the align module within Cerius.[2] Based on the assumption that each compound exerts activity at the same binding site on DNA, the structures of **5a–r** were aligned in a pharmacologically active

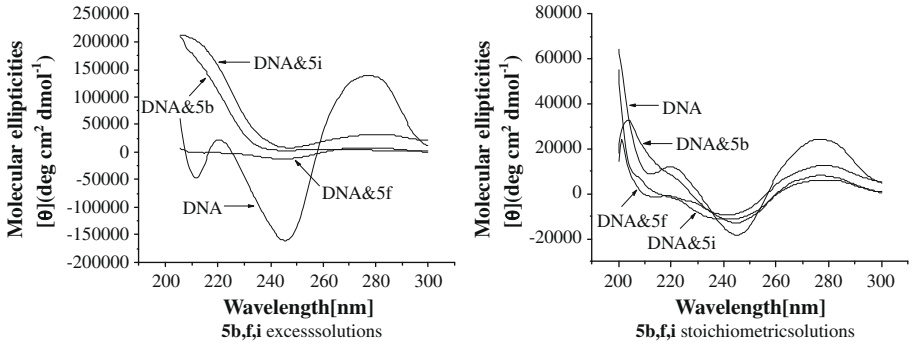

Figure 5. Effect of **5b**,**f**,**i** on the CD signals of CT DNA.

orientation. To obtain a consistent alignment, the 1,3-dithiolan-1-ylaldehyde moiety was selected as a common pharmacophore for the template to superimpose **5a–r**. The method used for performing the alignment was the maximum common subgraph (MCS). MCS looks at molecules as points and lines, and uses techniques from graph theory to identify patterns.[30] A rigid fit of atom pairings was performed to superimpose each structure onto the target model 1,3-dithiolan-1-ylaldehyde. A stereoview of aligned **5a–r** used for molecular field generation is shown in Figure 6.

2.4.2. QSAR module of Cerius² based MFA of 5a–r

After energy-minimization using MMFF94 (Merck Molecular Force Field), Molecular Field Analysis (MFA) was performed using the QSAR module of Cerius.[231] A five-step procedure, which included generating conformers, minimizing energy, matching atoms and aligning molecules, setting preferences, and analyzing regression, was automatically performed by MFA. Molecular electrostatic and steric fields were created by using proton and methyl groups, respectively, as probes. These fields were sampled at each point of a regularly spaced grid of 1 Å. An energy cut-off of ±30.0 kcal/mol was set for both electrostatic and steric fields. Totally, 672 grid points were generated. Although spatial and structural descriptors such as dipole moment, polarizability, radius of gyration, number of rotatable bonds, molecular volume, principal moment of inertia, AlogP98, number of hydrogen bond donors and acceptors, and molar refractivity were also considered, only the highest variance holder proton, methyl and hydroxyl descriptors were used. Regression analysis was carried out using the genetic partial least squares (G/PLS) method consisting of 50,000 generations with a population size of 100. The number of components was set to 5. Cross-validation was performed with the leave-one-out procedure. PLS analysis was scaled, with all variables normalized to a variance of 1.0.

2.4.2.1. MFA model for tumor weights of the mice receiving 5a–r.

Eq. 1 expresses the MFA model for predicted tumor weights of the mice receiving **5a–r** in terms of the descriptors proton, methyl, and hydroxyl groups (alignment shown in Fig. 7). Figure 8 shows the straight-line correlation of the actual tumor weights found in the S180 mouse model with the tumor weights calculated using Eq. 1.

$$\begin{aligned}\text{Activity} = {} & 21.46 + 0.91(\text{H}^+/953) - 0.32(\text{H}^+/956) \\ & - 0.30(\text{CH}_3/204) + 0.82(\text{CH}_3/401) + 0.27(\text{CH}_3/641) \\ & + 1.54(\text{CH}_3/710) + 0.16(\text{HO}^-/548) - 0.70(\text{HO}^-/577) \\ & - 0.31(\text{HO}^-/625) - 0.21(\text{HO}^-/760) - 0.21(\text{HO}^-/807) \\ & - 0.25(\text{HO}^-/891) - 0.23(\text{HO}^-/938) \end{aligned} \quad (1)$$

In Eq. 1, the data points (n), correlation coefficient (r), square correlation coefficient (r^2), cross-validated correlation coefficient (r^2cv), bootstrap correlation coefficient (r^2_{BS}) and least square error (LSE) were 18, 0.996, 0.992, 0.077, 0.213 and 3.029, respectively. The equation contains one term of H^+/953 with a positive coefficient, which means that an electron-donating group at this position will increase tumor inhibition, and one term of H^+/956 with a negative coefficient, which means that electron-withdrawing groups at this position will increase tumor inhibition. Eq. 1 includes three terms of CH_3/401, CH_3/641 and CH_3/710 with positive coefficients, which means that a large group at these sites will increase tumor inhibition, and one term of CH_3/204 with a negative coefficient, which means that a large group at this site will decrease tumor inhibition. Eq. 1 also contains one term of HO^-/548 with a positive coefficient, which means that an electron-donating group at this position will increase tumor inhibition, and six terms of HO^-/577, HO^-/625, HO^-/760, HO^-/807, HO^-/891 and HO^-/938 with negative coefficients, which means that electron-withdrawing groups at these positions will increase tumor inhibition.

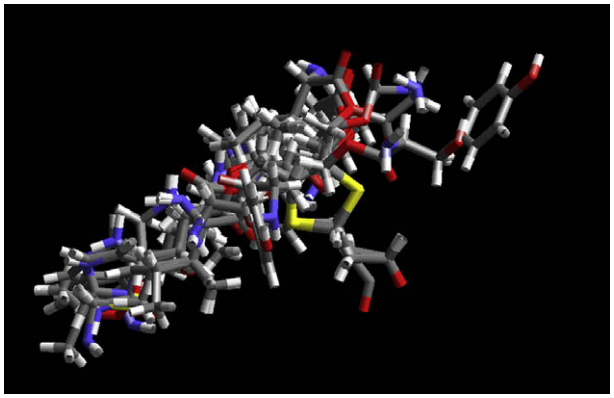

Figure 6. Alignment stereoview of **5a–r** used for molecular field generation.

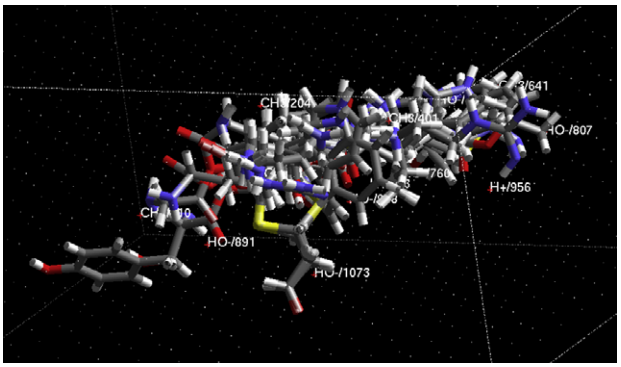

Figure 7. Alignment stereoview of **5a–r** reflecting tumor inhibition in mice.

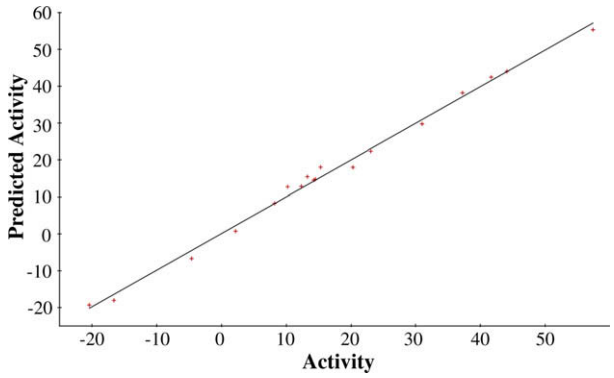

Figure 8. Graph of tested tumor weight against predicted tumor weight of mice receiving **5a**–**r**.

Examples of these factors are shown Figure 9. Compounds **5k,p** (A), which have electron-releasing groups near H^+/953 and HO^-/625, electron-withdrawing groups near HO^-/938, large groups near CH_3/401 and CH_3/641, and small groups near CH_3/204 showed increased antitumor activity, and **5d,f** (B), which have electron-withdrawing groups near H^+/956 and HO^-/548, and small groups near CH_3/641 and CH_3/401 showed significantly decreased tumor inhibition activity.

3. Conclusion

In summary, 18 *cis*-2-carbonylmethyl-4,5-di-L-aminoacyloxymethyl)-1,3-dithiolanes (**5a–r**) were synthesized from *cis*-2-carbonylmethyl-4,5-dihydroxymethyl-1,3-dithiolane and L-amino acids in this study. In an in vivo antitumor assay in S180 mice model, **5e,k,p** (AA = Gly, L-Phe or L-Tyr) exhibited the highest antitumor potency. In addition, the in vivo activity of **5e,k,p** at 44.64 μmol/kg were comparable to that of cytarabine at 89.28 μmol/kg. Compounds whose amino acid residues contain aromatic rings had the greatest antitumor activity. To explore the possible molecular target of the newly synthesized analogs, UV–vis and CD spectra were performed. Results from both studies demonstrated that DNA was the target of these compounds. A 3D QSAR model was also established in this study, and an equation with r^2 equal 0.992 was built to predict the in vivo antitumor activity of unknown *cis*-2,4,5-trisubstituted-1,3-dithiolane analogs.

4. Experimental

4.1. General

Statistical analysis of all biological data was carried out by use of ANOVA test with $p < 0.05$ as significant cut-off. Protected amino acids with L-configuration used were purchased from Sigma Chemical Co. All coupling and deprotective reactions were carried out under anhydrous conditions. Chromatography was performed on Qingdao Silica Gel H. The purity of the intermediates and the products was measured on TLC (Merck silica gel plates of type 60 F_{254}, 0.25 mm layer thickness) and HPLC (Waters, C_{18} column 4.6 × 150 mm). Melting points were determined in capillary tubes on an electrothermal SM/XMP apparatus without correction. UV spectra were measured on Shimadzu UV 2550. ESI-MS was determined by Micromass Quattro micro TM API, Waters Co. ^1H (300 and 500 MHz) and ^{13}C (75 and 125 MHz) NMR spectra were recorded on Bruker AMX-300 and AMX-500 spectrometers for DMSO-d_6 solution or $CDCl_3$ solution with tetramethylsilane as internal standard. Optical rotations were determined on P-1020 Jasco instrument.

Table 3
Chemical, physical and related data of **4a**–**r**

	Yield (%)	Mp (°C)	$[\alpha]_D^{25}$ (*c* 1.0, CH_3OH)	ESI-MS $[M+H]^+$
4a	91	Oil	−23.41	597
4b	43	101–104	−29.16	1167
4c	16	Oil	−46.56	683
4d	94	Oil	−46.49	711
4e	82	Oil	2.70	569
4f	73	71–72	−21.70	929
4g	84	Oil	−60.71	681
4h	73	Oil	−41.76	681
4 i	85	98–101	−60.99	911
4j	88	Oil	−17.57	717
4k	91	113–115	−9.48	749
4l	74	102–103	−92.15	649
4m	48	Oil	−45.23	629
4n	55	61–62	−15.96	657
4o	73	Oil	−33.37	653
4p	82	Oil	−50.07	981
4q	79	Oil	21.63	825
4r	81	Oil	−20.93	827

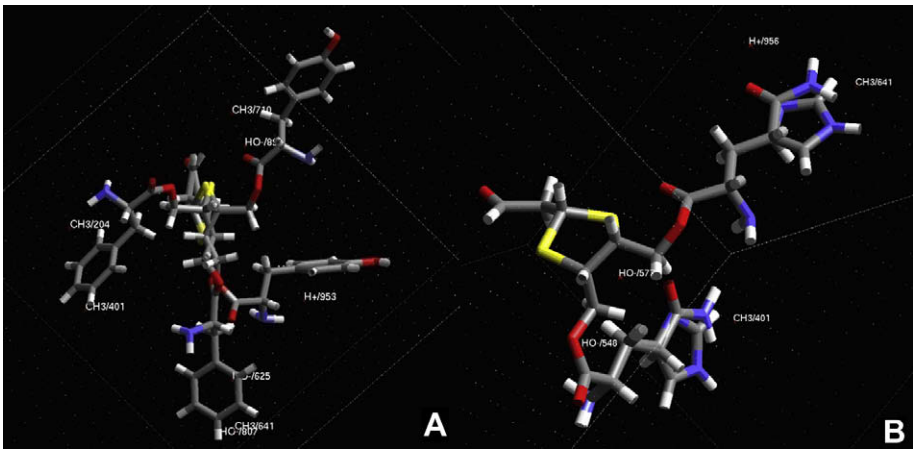

Figure 9. Electrostatic and steric environments of **5k**,**p** (A) and **5d**,**f** (B) within the grid with 3D points of Eq. 1.

Table 4
Elementary analysis data of **4a–r**

	Formula	Calcd			Found		
		C	H	N	C	H	N
4a	$C_{25}H_{44}N_2O_{10}S_2$	50.32	7.43	4.69	50.11	7.30	4.44
4b	$C_{51}H_{90}N_8O_{18}S_2$	52.47	7.77	9.60	52.69	7.91	9.85
4c	$C_{27}H_{46}N_4O_{12}S_2$	47.49	6.79	8.21	47.71	6.94	7.97
4d	$C_{29}H_{50}N_4O_{12}S_2$	49.00	7.09	7.88	49.23	7.22	8.14
4e	$C_{23}H_{40}N_2O_{10}S_2$	48.57	7.09	4.93	48.35	6.96	4.70
4f	$C_{41}H_{64}N_6O_{14}S_2$	53.00	6.94	9.05	52.77	6.80	8.81
4g	$C_{31}H_{56}N_2O_{10}S_2$	54.68	8.29	4.11	54.46	8.15	4.35
4h	$C_{31}H_{56}N_2O_{10}S_2$	54.68	8.29	4.11	54.89	8.42	4.34
4i	$C_{41}H_{74}N_4O_{14}S_2$	54.04	8.19	6.15	53.83	8.04	6.38
4j	$C_{29}H_{52}N_2O_{10}S_4$	48.58	7.31	3.91	48.36	7.20	3.66
4k	$C_{37}H_{52}N_2O_{10}S_2$	59.34	7.00	3.74	59.55	7.16	3.98
4l	$C_{29}H_{48}N_2O_{10}S_2$	53.68	7.46	4.32	53.46	7.33	4.10
4m	$C_{25}H_{44}N_2O_{12}S_2$	47.76	7.05	4.46	47.54	6.91	4.69
4n	$C_{27}H_{48}N_2O_{12}S_2$	49.37	7.37	4.27	49.42	7.29	4.23
4o	$C_{29}H_{52}N_2O_{10}S_2$	53.35	8.03	4.29	53.12	7.90	4.03
4p	$C_{47}H_{68}N_2O_{16}S_2$	57.53	6.99	2.86	57.30	6.84	3.13
4q	$C_{37}H_{64}N_2O_{14}S_2$	53.86	7.82	3.40	53.65	7.70	3.65
4r	$C_{41}H_{54}N_4O_{10}S_2$	59.54	6.58	6.77	59.31	6.44	6.53

4.2. Synthesis

4.2.1. *cis*-2-(2,2-Dimethoxyethyl)-4,5-dimethoxycarbonyl-1,3-dithiolane (2)

To a solution of 1.81 g (11.0 mmol) of 1,1,3,3-tetra-methoxypropane (TMOP) and 2.1 g (10.0 mmol) of dimethyl (2*R*,3*S*)-2,3-dimercaptosuccinate in 50 mL of $CHCl_3$, 1 mL of concentrated HCl was added. The mixture was stirred at 40 °C for 48 h. TLC analysis ($CHCl_3$/MeOH/HOAc, 10/1/0.2) indicated complete disappearance of starting materials. The mixture was neutralized with saturated aqueous solution of $NaHCO_3$ to pH 7 and extracted with water three times. The organic layer was dried over anhydrous Na_2SO_4 overnight, and then filtered. The filtrate was evaporated under vacuum to give 3.70 g of yellow oil, which was purified by chromatography on silica gel (petroleum ether–EtOAc, 3:1) to yield 2.4 g (77%) of the title compound as colorless oil. ESI-MS (*m/e*): 311 $[M+H]^+$. ^1H NMR ($CDCl_3$): δ 4.63 (t, J = 7.0 Hz, 1H), 4.49 (d, J = 8.0 Hz, 2H), 4.41 (t, J = 6.0 Hz, 1H), 3.77 (s, 6H), 3.35 (s, 6H), 2.14 (t, J = 7.0 Hz, 2H). Anal. Calcd for $C_{11}H_{18}O_6S_2$: C, 42.57; H, 5.85. Found: C, 42.80; H, 5.71.

Table 5
1H NMR data of **4a–r** except R

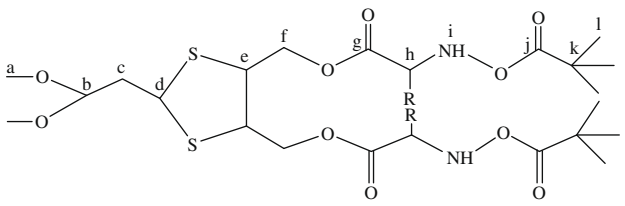

	Ha	Hb	Hc	Hd	He	Hf	Hh	Hi	Hl
4a	3.35, 6H, s	4.55, 1H, t, J = 7.0	2.15, 2H, t, J = 5.5	4.44, 1H, t, J = 6.0	4.33, 2H, t, J = 8.5	4.40, 4H, d, J = 7.0	3.92, 2H, m, J = 9.0	5.25, 5.13, 2H, s	1.46 18H, s
4b	3.35, 6H, s	4.51, 1H, t, J = 7.0	2.14, 2H, t, J = 5.5	4.42, 1H, t, J = 8.0	4.31, 2H, t, J = 7.5	4.40, 4H, m	3.86, 2H, m, J = 5.5	5.62, 5.55, 2H, s	1.45 18H, s
4c	3.29, 6H, s	4.52, 1H, t, J = 6.5	2.13, 2H, t, J = 6.0	4.41, 1H, t, J = 6.0	4.33, 2H, t, J = 6.0	4.36, 4H, t, J = 5.0	3.90, 2H, m, J = 5.5	5.81, 5.63, 2H, s	1.43 18H, s
4d	3.29, 6H, s	4.53, 1H, t, J = 6.5	2.13, 2H, t, J = 6.0	4.42, 1H, t, J = 5.5	4.33, 2H, t, J = 6.5	4.37, 4H, t, J = 5.5	3.90, 2H, m, J = 5.5	5.82, 5.65, 2H, s	1.43 18H, s
4e	3.33, 6H, s	4.53, 1H, t, J = 7.0	2.14, 2H, t, J = 6.0	4.42, 1H, t, J = 6.0	3.87, 2H, t, J = 5.0	4.36, 4H, t, J = 7.0	3.90, 4H, t, J = 4.5	5.24, 2H, s	1.44 18H, s
4f	3.35, 6H, s	4.55, 1H, t, J = 7.0	2.13, 2H, t, J = 6.0	4.42, 1H, t, J = 6.0	4.32, 2H, q, J = 6.5	4.39, 4H, t, J = 7.0	3.90, 2H, m, J = 5.0	7.24, 7.11, 2H, s	1.46 18H, s
4g	3.36, 6H, s	4.57, 1H, t, J = 7.0	2.15, 2H, t, J = 6.5	4.44, 1H, t, J = 6.0	4.27, 2H, q, J = 6.0	4.40, 4H, t, J = 6.5	3.90, 2H, q, J = 7.5	5.22, 5.08, 2H, s	1.46 18H, s
4h	3.33, 6H, s	4.50, 1H, t, J = 7.0	2.13, 2H, t, J = 6.5	4.40, 1H, t, J = 6.0	4.25, 2H, q, J = 6.0	4.36, 4H, t, J = 8.5	3.88, 2H, q, J = 6.0	5.27, 5.00, 2H, s	1.43 18H, s
4i	3.35, 6H, s	4.54, 1H, t, J = 7.0	2.34, 2H, t, J = 6.5	4.45, 1H, m	3.94, 2H, m, J = 5.5	4.36, 4H, d, J = 6.5	3.90, 2H, q, J = 7.0	5.40, 5.24, 2H, s	1.46 18H, s
4j	3.34, 6H, s	4.55, 1H, t, J = 7.0	2.15, 2H, t, J = 6.5	4.41, 1H, t, J = 7.0	3.96, 2H, m, J = 6.5	4.38, 4H, d, J = 6.0	3.90, 2H, m, J = 6.5	5.43, 5.25, 2H, s	1.44 18H, s
4k	3.36, 6H, s	4.56, 1H, t, J = 7.0	2.16, 2H, t, J = 5.0	4.45, 1H, t, J = 6.5	4.34, 2H, m, J = 8.0	4.41, 4H, d, J = 6.0	3.91, 2H, m, J = 5.0	5.26, 5.14, 2H, s	1.46 18H, s
4l	3.35, 6H, s	4.55, 1H, t, J = 6.5	2.16, 2H, t, J = 5.5	4.44, 1H, t, J = 4.5	4.29, 2H, q, J = 5.5	4.39, 4H, d, J = 5.0	3.90, 2H, m, J = 8.0	—	1.46 18H, s
4m	3.36, 6H, s	4.50, 1H, t, J = 6.0	2.13, 2H, t, J = 5.0	4.41, 1H, t, J = 5.0	4.23, 2H, m, J = 5.0	4.37, 4H, d, J = 6.0	3.90, 2H, m, J = 5.5	5.50, 5.40, 2H, s	1.46 18H, s
4n	3.36, 6H, s	4.52, 1H, t, J = 7.0	2.13, 2H, t, J = 5.0	4.41, 1H, t, J = 5.0	4.23, 2H, q, J = 4.0	4.37, 4H, d, J = 6.0	3.90, 2H, q, J = 6.0	5.50, 5.41, 2H, s	1.46 18H, s
4o	3.36, 6H, s	4.56, 1H, t, J = 7.0	2.16, 2H, t, J = 6.0	4.44, 1H, t, J = 5.5	4.25, 2H, q, J = 4.5	4.40, 4H, d, J = 6.5	3.91, 2H, q, J = 7.0	5.21, 5.07, 2H, s	1.46 18H, s
4p	3.35, 6H, s	4.54, 1H, t, J = 7.5	2.15, 2H, t, J = 6.5	4.52, 1H, t, J = 8.5	4.30, 2H, q, J = 5.5	4.45, 4H, d, J = 6.0	3.79, 2H, m	5.26, 5.11, 2H, s	1.42 18H, s
4q	3.51, 6H, s	4.54, 1H, t, J = 7.0	2.15, 2H, t, J = 9.5	4.15, 1H, t, J = 9.0	4.34, 2H, m	4.37, 4H, m, J = 9.0	3.86, 2H, m, J = 7.5	5.42, 5.28, 2H, s	1.44 18H, s
4r	3.31, 6H, s	4.53, 1H, t, J = 7.0	2.02, 2H, t, J = 6.0	4.38, 1H, t, J = 6.0	3.88, 2H, q, J = 6.0	4.32, 4H, m, J = 7.0	3.72, 2H, m, J = 7.5	5.42, 5.28, 2H, s	1.46 18H, s

Table 6
NMR data of R in **4a–r**

	Structure of R[a]	^{1}H	^{13}C
4a	CH_3	1.42 (d, *J* = 7.0, 6H)	18.36
4b	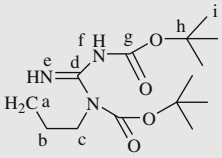	a: 1.84 (m, 4H); b: 1.28 (m, *J* = 7.0, 4H); c: 3.48 (m, *J* = 4.5, 4H); d: 9.31 (s, 2H); f: g: 9.44 (s, 2H); j: 1.53 (s, 36H)	a: 28.34; j: 28.19; b: 22.08; c: 39.11; e: 158.86; h: 155.13, 154.59; i: 79.83, 79.66
4c	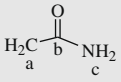	a: 2.72 (d, *J* = 5.5, 4H); c: 6.58 (s, 2H), 6.14 (s, 2H)	a: 36.71; b: 175.42
4d	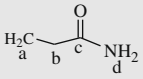	a: 1.25 (m, *J* = 3.0, 4H); b: 2.37 (t, *J* = 4.5, 4H); d: 6.60 (s, 2H), 6.16 (s, 2H)	a: 27.38; b: 33.84; c: 176.13
4f	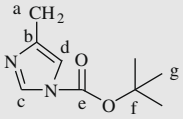	a: 2.94 (dd, *J* = 11.5, *J* = 3.5, 4H); c: 7.49 (s, 2H); d: 6.88 (s, 2H); g: 1.46 (s, 18H)	a: 34.59; b: 126.75; c: 134.66; d: 118.83; e: 151.22; f: 80.03; g: 27.21
4g	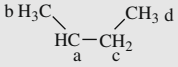	a: 1.90 (m, *J* = 3.0, 2H); b: 0.96 (d, *J* = 8.0, 6H); c: 1.24 (q, *J* = 9.0, 4H); d: 0.94 (t, *J* = 3.5, 6H)	a: 37.78; b: 15.65; c: 25.02; d: 11.57
4h	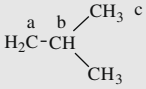	a: 1.58 (m, *J* = 3.0, 4H); b: 1.64 (m, *J* = 3.0, 2H); c: 0.94 (d, *J* = 7.5, 12H)	a: 24.82; b: 41.48; c: 22.87
4i	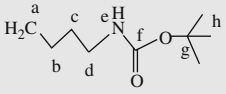	a: 1.84 (m, *J* = 7.0, 4H); b: 1.66 (m, 4H); c: 1.72 (m, 4H); d: 3.14 (m, 4H); e: 4.78 (s, 1H), 4.74 (s, 1H); h: 1.46 (s, 18H)	a: 31.02; b: 22.67; c: 29.57; d: 41.53; f: 155.62; g: 79.59; h: 21.71
4j	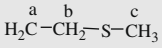	a: 1.97 (q, *J* = 7.5, 4H); b: 2.56 (t, *J* = 5.5, 4H); c: 2.11 (s, 6H)	a: 31.79; b: 30.07; c: 15.47
4k	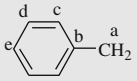	a: 2.89 (dd, *J* = 10.5, *J* = 4.5, 4H); c: 7.24 (d, *J* = 8.5, 4H), d: 7.16 (d, *J* = 4.0, 4H); e: 7.27 (t, *J* = 4.5, 2H);	a: 38.18; b: 135.96; c: 127.11; d: 128.64; e: 129.31
4l		b: 2.00 (m, *J* = 7.0, 4H); c: 1.89 (m, *J* = 5.5, 4H); d: 2.25 (m, *J* = 8.0, 4H)	b: 29.90; c: 23.63; d: 42.61
4m		a: 4.13 (m, 4H); b: 4.55 (s, 2H)	a: 60.77
4n	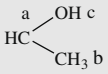	a: 4.34 (m, 2H); b: 1.33 (d, *J* = 5.5, 6H); c: 4.59 (s, 2H)	a: 70.74; b: 24.57
4o	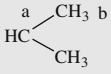	a: 2.14 (m, *J* = 6.0, 2H); b: 1.00 (d, *J* = 7.5, 6H), 0.90 (d, *J* = 7.5, 6H)	a: 31.08; b: 17.10
4p	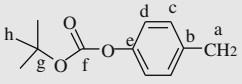	a: 3.14 (dd, *J* = 8.0, *J* = 5.0, 4H); c: 7.14 (d, *J* = 8.0, 4H); d: 7.12 (d, *J* = 8.0, 4H); h: 1.57 (s, 18H)	a: 37.52; b: 133.63; c: 121.45; d: 130.27; e: 150.18; f: 151.83; g: 83.54; h: 24.84
4q	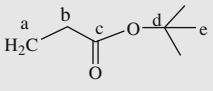	a: 2.24 (m, *J* = 7.0, 4H); b: 2.51 (t, *J* = 12.5, 4H); e: 1.42 (s, 18H)	a: 27.30; b: 30.30; c: 172.48; d: 82.1; e: 29.80
4r	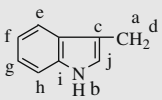	a: 3.24 (dd, *J* = 12.0, *J* = 4.0, 4H); b: 9.11 (s, 1H), 9.05 (s, 1H); e: 7.55 (d, *J* = 7.0, 2H), g: 7.36 (d, *J* = 8.0, 2H), f and h: 7.17 (m, *J* = 4.5, 4H); j: 7.00 (d, 2H)	a: 30.89; c: 109.25; d: 127.26; e: 118.77; f: 119.78; g: 122.31; h: 111.65; i: 136.23; j: 123.36

[a] Compound **4e** has no R.

Table 7
^{13}C NMR data of **4a–r** except R

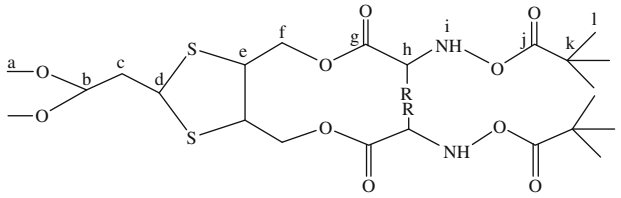

	Ca	Cb	Cc	Cd	Ce	Cf	Cg	Ch	Cj	Ck	Cl
4a	53.47	103.42	46.12	40.94	47.15	63.91	172.81	49.30	155.18	80.02	28.33
4b	55.47	103.28	46.37	40.93	47.22	64.01	173.03	53.56	155.88	80.03	28.34
4c	53.21	103.23	46.53	40.75	47.29	63.66	171.93	50.40	155.90	80.07	28.23
4d	53.89	103.17	46.29	40.44	47.48	63.59	171.94	53.34	155.58	79.44	28.41
4e	53.43	103.45	45.76	40.42	46.18	63.67	171.88	47.39	155.66	79.89	28.22
4f	55.46	103.37	46.33	40.72	47.84	63.49	172.14	54.01	155.47	79.97	28.33
4g	54.24	103.45	46.27	41.02	47.31	63.83	171.84	53.44	155.65	79.90	28.32
4h	53.56	103.48	45.94	40.35	47.12	63.77	172.51	52.92	155.56	79.90	28.32
4i	54.06	103.43	46.33	40.29	47.24	63.54	172.24	53.38	156.11	80.02	28.33
4j	53.48	103.39	46.11	40.92	47.15	63.92	171.80	52.89	155.48	80.07	28.31
4k	54.73	103.42	46.23	40.87	47.25	63.64	171.35	53.56	155.17	80.05	28.28
4l	53.70	103.46	46.33	41.00	47.46	65.80	172.32	63.90	154.36	79.95	28.39
4m	53.41	103.44	45.35	45.35	47.22	63.15	171.02	57.11	155.73	80.08	28.40
4n	53.69	103.37	44.75	40.81	47.27	63.99	170.50	58.42	156.11	79.90	28.31
4o	53.41	103.44	46.26	41.00	47.29	63.78	171.82	58.59	155.73	79.90	28.31
4p	54.71	103.44	46.18	40.86	47.23	63.77	171.38	53.35	155.19	80.16	28.29
4q	54.01	103.41	46.39	40.93	47.10	63.92	171.61	53.57	155.82	80.15	28.30
4r	53.51	103.31	46.57	40.82	47.41	63.76	172.06	56.12	156.08	80.11	28.46

Table 8
Chemical, physical and related data of **5a–r**

	Yield (%)	Mp (°C)	$[\alpha]_D^{25}$ (*c* 1.0, H_2O)	ESI-MS $[M+H]^+$
5a	91	151–153	−14.63	351
5b	95	132–133	9.14	521
5c	90	170–172	11.70	437
5d	93	181–183	6.37	465
5e	89	181–182	6.50	323
5f	97	202–204	15.40	483
5g	98	175–176	6.03	435
5h	90	165–166	3.30	435
5i	91	124–126	14.09	465
5j	97	154–155	10.16	471
5k	96	168–169	3.90	503
5l	97	Oil	−16.80	403
5m	92	176–178	2.97	383
5n	93	150–151	−16.33	411
5o	94	166–167	1.50	407
5p	94	121–122	5.00	535
5q	94	143–145	3.77	467
5r	95	>220	6.47	581

Table 9
Elementary analysis data of **5a–r**

	Formula	Calcd			Found		
		C	H	N	C	H	N
5a	$C_{13}H_{22}N_2O_5S_2$	44.55	6.33	7.99	44.34	6.20	7.75
5b	$C_{19}H_{36}N_8O_5S_2$	43.83	6.97	21.52	43.05	6.81	21.77
5c	$C_{15}H_{24}N_4O_7S_2$	41.27	5.54	12.84	41.51	5.70	12.60
5d	$C_{17}H_{28}N_4O_7S_2$	43.95	6.08	12.06	43.72	5.93	12.31
5e	$C_{11}H_{18}N_2O_5S_2$	40.98	5.63	8.69	40.77	5.50	8.92
5f	$C_{19}H_{26}N_6O_5S_2$	47.29	5.43	17.41	47.50	5.59	17.66
5g	$C_{19}H_{34}N_2O_5S_2$	52.51	7.89	6.45	52.30	7.74	6.69
5h	$C_{19}H_{34}N_2O_5S_2$	52.51	7.89	6.45	52.28	7.72	6.69
5i	$C_{19}H_{36}N_4O_5S_2$	49.11	7.81	12.06	48.90	7.66	12.32
5j	$C_{17}H_{30}N_2O_5S_4$	43.38	6.42	5.95	43.14	6.28	5.71
5k	$C_{25}H_{30}N_2O_5S_2$	59.74	6.02	5.57	59.95	6.17	5.84
5l	$C_{17}H_{26}N_2O_5\ S_2$	50.72	6.51	6.96	50.50	6.37	6.70
5m	$C_{13}H_{22}N_2O_7S_2$	40.83	5.80	7.32	40.60	5.94	7.10
5n	$C_{15}H_{26}N_2O_7S_2$	43.89	6.38	6.82	43.66	6.21	6.60
5o	$C_{17}H_{30}N_2O_5S_2$	50.22	7.44	6.89	50.00	7.28	7.14
5p	$C_{25}H_{30}N_2O_7S_2$	56.16	5.66	5.24	56.38	5.80	5.49
5q	$C_{17}H_{26}N_2O_9S_2$	43.77	5.62	6.00	43.54	5.50	6.26
5r	$C_{29}H_{32}N_4O_5S_2$	59.98	5.55	9.65	59.74	5.41	9.91

4.2.2. *cis*-2-(2,2-Dimethoxyethyl)-4,5-dihydroxymethyl-1,3-dithiolane (3)

A suspension of 432 mg (12.0 mmol) of $LiAlH_4$ in 30 mL of anhydrous THF was stirred vigorously at 40 °C for 1 h, after which a solution of 1.70 g (5.0 mmol) of **2** in 20 mL of anhydrous THF was added. The reaction was continued for 4 h, at which time TLC analysis (petroleum ether–EtOAc, 3:1) indicated complete disappearance of **2**. The reaction mixture was stirred vigorously, cooled in an ice bath, quenched by slowly adding crushed ice, and neutralized by adding a solution of 2 mL of concentrated hydrochloric acid in 30 mL of water. The formed suspension was filtered, the filtrate was evaporated under vacuum, the residue was extracted with EtOAc (30 mL × 3), and the organic layer was washed successively with satd aq NaCl, aq $NaHCO_3$ (5%), and satd aq NaCl. The organic layer was dried over anhydrous Na_2SO_4 and filtered, and the filtrate was evaporated under vacuum to give a colorless oil, which was purified by chromatography on silica gel ($CHCl_3$–MeOH, 40:1) to yield 1.24 g (80%) of the title compound as colorless oil. ESI-MS (*m/e*): 255 $[M+H]^+$. ^{1}H NMR ($CDCl_3$) δ 5.01 (t, *J* = 5.0 Hz, 2H), 4.43 (t, *J* = 7.0 Hz, 1H), 3.76 (d, *J* = 5.0 Hz, 4H), 3.73 (t, *J* = 5.0 Hz, 1H), 3.49 (t, *J* = 5.0 Hz, 2H), 3.35 (s, 6H), 2.15 (t, *J* = 7.0 Hz 2H). Anal. Calcd for $C_9H_{18}O_4S_2$: C, 42.50; H, 7.13. Found: C, 42.81; H, 7.00.

4.2.3. General procedure for preparing *cis*-2-(2,2-dimethoxyethyl)-4,5-di(*N*-Boc-L-aminoacy-loxymethyl)-1,3-dithiolanes (4a–r)

A solution of 254 mg (1.0 mmol) of **3**, 2.2 mmol of Boc-L-amino acid, 453 mg (2.2 mmol) of DCC and 26.8 mg (0.22 mmol) of DMAP in 20 mL of anhydrous CH_2Cl_2 was stirred at room temperature for 0.5 h. TLC analysis (petroleum ether–EtOAc, 3:1) indicated complete

Table 10
^{1}H NMR data of **5a–r** except R

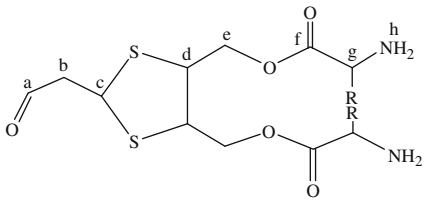

	Ha	Hb	Hc	Hd	He	Hg	Hh
5a	9.58, 1H, s	3.09, 2H, dd, *J* = 10.5, *J* = 3.0	4.24, 1H, t, *J* = 6.0	3.74, 2H, m, *J* = 5.0	4.28, 4H, d, *J* = 5.0	3.82, 2H, m, *J* = 7.0	8.71, 4H, s
5b	9.59, 1H, s	2.88, 2H, dd, *J* = 11.5, *J* = 3.0	4.38, 1H, t, *J* = 5.0	4.07, 2H, m, *J* = 6.0	4.47, 4H, d, *J* = 6.0	4.25, 2H, m, *J* = 3.0	8.72, 4H, s
5c	9.58, 1H, s	3.10, 2H, dd, *J* = 10.0, *J* = 3.0	4.24, 1H, t, *J* = 6.0	3.74, 2H, m, *J* = 5.0	4.28, 4H, , d, *J* = 5.0	3.84, 2H, m, *J* = 7.0	8.71, 4H, s
5d	9.60, 1H, s	3.08, 2H, dd, *J* = 10.5, *J* = 3.0	4.30, 1H, t, *J* = 6.5	3.82, 2H, m, *J* = 5.5	4.34, 4H, d, *J* = 5.5	4.21, 2H, m, *J* = 5.5	8.73, 4H, s
5e	9.60, 1H, s	3.09, 2H, dd, *J* = 10.5, *J* = 3.0	4.24, 1H, t, *J* = 6.0	3.83, 2H, m, *J* = 5.0	4.26, 4H, d, *J* = 7.0	3.88, 4H, m, *J* = 5.5	8.67, 4H, s
5f	9 58, 1H, s	3.10, 2H, dd, *J* = 11.5, *J* = 3.0	4.23, 1H, t, *J* = 6.5	3.74, 2H, m, *J* = 6.0	4.27, 4H, d, *J* = 6.0	3.82, 2H, m, *J* = 7.0	9.00, 4H, s
5g	9.59, 1H, s	3.12, 2H, dd, *J* = 10.5, *J* = 2.5	4.34, 1H, t, *J* = 6.0	3.92, 2H, m, *J* = 4.5	4.37, 4H, d, *J* = 7.0	4.08, 2H, m, *J* = 6.5	8.74, 4H, s
5h	9.59, 1H, s	3.10, 2H, dd, *J* = 10.0, *J* = 3.0	4.29, 1H, t, *J* = 6.5	3.82, 2H, m, *J* = 5.0	4.34, 4H, d, *J* = 7.0	3.9, 2H, m, *J* = 6.5	8.73, 4H, s
5i	9.59, 1H, s	3.10, 2H, m	4.22, 1H, t, *J* = 6.5	3.80, 2H, , m, *J* = 7.0	4.26, 4H, d, *J* = 6.5	3.99, 2H, m, *J* = 5.5	8.84, 4H, s
5j	9.58, 1H, s	3.10, 2H, m	4.33, 1H, t, *J* = 6.0	3.90, 2H, m, *J* = 6.5	4.38, 4H, d, *J* = 6.0	4.01, 2H, m, *J* = 5.0	8.71, 4H, s
5k	9.58, 1H, s	3.19, 2H, dd, *J* = 11.5, *J* = 5.0	4.23, 1H, t, *J* = 7.0	3.74, 2H, m, *J* = 6.0	4.27, 4H, d, *J* = 5.0	3.82, 2H, m, *J* = 8.0	8.71, 4H, s
5l	9.58, 1H, s	3.15, 2H, dd, *J* = 11.5, *J* = 5.0	4.34, 1H, t, *J* = 7.5	3.94, 2H, m, *J* = 5.5	4.48, 4H, d, *J* = 7.0	4.31, 2H, m, *J* = 6.0	8.70, 2H, s
5m	9.58, 1H, s	3.09, 2H, dd, *J* = 10.5, *J* = 3.0	4.23, 1H, t, *J* = 6.0	3.74, 2H, m, *J* = 5.0	4.28, 4H, d, *J* = 5.0	3.83, 2H, m, *J* = 7.0	8.71, 4H, s
5n	9.58, 1H, s	3.09, 2H, dd, *J* = 9.5, *J* = 3.5	4.22, 1H, t, *J* = 6.5	3.74, 2H, m	4.28, 4H, d, *J* = 5.0	3.88, 2H, m, *J* = 5.0	8.71, 4H, s
5o	9.58, 1H, s	3.09, 2H, m, *J* = 7.0	4.34, 1H, t, *J* = 5.5	3.91, 2H, m, *J* = 7.0	4.38, 4H, d, *J* = 6.5	4.25, 2H, m, *J* = 4.5	8.70, 4H, s
5p	9.58, 1H, s	3.09, 2H, dd, *J* = 10.0, *J* = 6.5	4.25, 1H, t, *J* = 6.5	3.98, 2H, m, *J* = 5.5	4.29, 4H, d, *J* = 5.5	4.43, 2H, m	8.73, 4H, s
5q	9.59, 1H, s	3.12, 2H, dd, *J* = 10.5, *J* = 2.5	4.34, 1H, t, *J* = 6.0	3.92, 2H, m, *J* = 4.5	4.38, 4H, d, *J* = 6.5	4.08, 2H, m, *J* = 6.5	8.77, 4H, s
5r	9.58, 1H, s	3.06, 2H, dd, *J* = 10.0, *J* = 4.5	4.04, 1H, t, *J* = 10.0	3.87, 2H, m	4.25, 4H, d, *J* = 6.0	3.98, 2H, m, *J* = 3.5	8.70, 4H, s

disappearance of **3**. The reaction mixture was filtered, the filtrate was washed successively with satd aq NaCl, aq $NaHCO_3$ (5%), aq $KHSO_4$ (5%), and satd aq NaCl. The organic layer was dried over anhydrous Na_2SO_4 and filtered. The filtrate was evaporated under vacuum to give colorless oil, which was purified by silica gel chromatography (petroleum ether–EtOAc, 5:1) to yield title compounds *cis*-2-(2,2-dimethoxyethyl)-4,5-di(*N*-Boc-L-alanyloxymethyl)-1,3-dithiolane (**4a**), *cis*-2-(2,2-dimethoxyethyl)-4,5-di(N^G,N^G,N^α-triBoc-L-arginyloxymethyl)-1,3-dithiolane (**4b**), *cis*-2-(2,2-dimethoxyethyl)-4,5-di(*N*-Boc-L-asparaginyloxymethyl)-1,3-dithiolane (**4c**), *cis*-2-(2,2-dimethoxyethyl)-4,5-di(*N*-Boc-L-glutaminyloxymethyl)-1,3-dithiolane (**4d**), *cis*-2-(2,2-dimethoxyethyl)-4,5-di(*N*-Boc-L-glycinyloxymethyl)-1,3-dithiolane (**4e**), *cis*-2-(2,2-dimethoxyethyl)-4,5-di(*N*,*N*-di-Boc-L-histidinyl-oxymethyl)-1,3-dithiolane (**4f**), *cis*-2-(2,2-dimethoxyethyl)-4,5-di(*N*-Boc-L-isoleucinyloxymethyl)-1,3-dithiolane (**4g**) *cis*-2-(2,2-dimethoxyethyl)-4,5-di(*N*-Boc-L-leucinyloxymethyl)-1,3-dithiolane (**4h**), *cis*-2-(2,2-dimethoxyethyl)-4,5-di(N^ω,N^α-diBoc-L-lysyloxymethyl)-1,3-dithiolane (**4i**), *cis*-2-(2,2-dimethoxyethyl)-4,5-di(*N*-Boc-L-methionyloxymethyl)-1,3-dithiolane (**4j**), *cis*-2-(2,2-dimethoxyethyl)-4,5-di(*N*-Boc-L-phenylalaninyloxymethyl)-1,3-dithiolane (**4k**), *cis*-2-(2,2-dimethoxyethyl)-4,5-di(*N*-Boc-L-prolinyloxymethyl)-1,3-dithiolane (**4l**), *cis*-2-(2,2-dimethoxyethyl)-4,5-di(*N*-Boc-L-serinyloxymethyl)-1,3-dithiolane (**4m**), *cis*-2-(2,2-dimethoxyethyl)-4,5-di(*N*-Boc-L-threoninyloxymethyl)-1,3-dithiolane (**4n**), *cis*-2-(2,2-dimethoxyethyl)-4,5-di(*N*-Boc-L-valinyloxymethyl)-1,3-dithiolane (**4o**), *cis*-2-(2,2-dimethoxyethyl)-4,5-di(*O*,*N*-diBoc-L-tyrosyloxymethyl)-1,3-dithiolane (**4p**), *cis*-2-(2,2-dimethoxyethyl)-4,5-di(*N*-Boc-γ-*tert*-butylester-L-glutamoyloxymethyl)-1,3-dithiolane (**4q**), and *cis*-2-(2,2-dimethoxyethyl)-4,5-di(*N*-Boc-L-tryptophanyloxymethyl)-1,3-dithiolane (**4r**). Their chemical, physical, spectral and elemental analysis data are listed in Tables 3–7.

4.2.4. General procedure for preparing *cis*-2-carbonylmethyl-4,5-di-L-amino-acyloxymethyl)-1,3-dithiolanes (5a–r)

At 0 °C, a solution of 0.1 mmol of **4a–r** in 5 mL of anhydrous EtOAc was treated with 15 mL of EtOAc containing HCl (6 M) and stirred for 1 h. TLC analysis ($CHCl_3$–MeOH, 10:1) indicated complete disappearance of **4a–r**. The reaction mixture was evaporated under vacuum to remove excess HCl, and the residue was triturated with anhydrous diethyl ether and then purified by silica gel chromatography ($CHCl_3$–MeOH, 25:1) to give *cis*-2-carbonylmethyl-4,5-di(L-alanyloxymethyl)-1,3- dithiolane (**5a**), *cis*-2-carbonylmethyl-4,5-di(L-arginyloxymethyl)-1,3-dithiolane (**5b**), *cis*-2-carbonylmethyl-4,5-di(L-asparaginyloxymethyl)-1,3-dithiolane (**5c**), *cis*-2- carbonylmethyl-4,5-di(L-glutaminyloxymethyl)-1,3-dithiolane (**5d**), *cis*-2-carbonyl-methyl-4,5-di(L-glycinyloxymethyl)-1,3-dithiolane (**5e**), *cis*-2-carbonylmethyl-4,5- di(N-Boc-L-histidinyloxymethyl)-1,3-dithiolane (**5f**), *cis*-2-carbonylmethyl-4,5-di(L-isoleucinyloxymethyl)-1,3-dithiolane (**5g**), *cis*-2-carbonylmethyl-4,5-di(L-leucinyl-oxymethyl)-1,3-dithiolane (**5h**), *cis*-2-carbonylmethyl-4,5-di(L-lysyloxymethyl)-1,3-dithiolane (**5i**), *cis*-2-carbonylmethyl-4,5-di(L-methionyloxymethyl)-1,3-dithiolane (**5j**), *cis*-2-carbonylmethyl-4,5-di(L-phenylalaninyloxymethyl)-1,3-dithiolane (**5k**), *cis*-2-carbonylmethyl-4,5-di(L-prolinyloxymethyl)-1,3-dithiolane (**5l**), *cis*-2-carbonylmethyl-4,5-di(L-serinyloxymethyl)-1,3-dithiolane (**5m**), *cis*-2-carbonylmethyl-4,5-di(L-threoninyloxymethyl)-1,3-dithiolane (**5n**), *cis*-2-carbonylmethyl-4,5-di(L-valinyloxymethyl)-1,3-dithiolane (**5o**), *cis*-2-carbonylmethyl-4,5-di(L-tyrosyloxymethyl)-1,3-dithiolane (**5p**), *cis*-2-carbonylethyl-4,5-di(L-glutamoyloxymethyl)-1,3-dithiolane (**5q**), and *cis*-2-carbonylmethyl-4,5-di(L-tryptophanyloxymethyl)-1,3-dithiolane (**5r**). Their chemical, physical, spectral and elemental analysis data are listed in Tables 8–12.

4.3. In vivo anticancer assay

Male ICR mice, purchased from Peking University Health Science Center, were maintained at 21 °C with a natural day/night cycle in a conventional animal colony. The mice were 10–12 weeks old at the beginning of the experiments. The tumor used was S180, which forms solid tumors when injected subcutaneously. S180 cells for initiation of subcutaneous tumors were obtained from the ascitic form of the tumors in mice, which were serially

Table 11
NMR data of R in **5a–r**

	Structure of R[a]	^{1}H	^{13}C
5a	CH_3	1.53 (d, *J* = 7.5, 6H)	20.62
5b	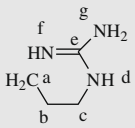	a: 3.20 (m, *J* = 5.5, 4H); b: 2.17 (m, *J* = 2.5, 4H); c: 4.02 (m, 4H); d: 8.98 (s, 2H); f: 9.44 (s, 2H); g: 8.44 (s, 4H)	a: 31.91; b: 25.08; c: 38.22; e: 158.86
5c	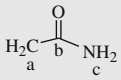	a: 2.72 (d, *J* = 5.5, 4H); c: 6.56 (s, 2H), 6.15 (s, 2H)	a: 34.76; b: 169.25
5d	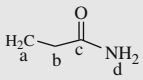	a: 1.55 (m, *J* = 3.0, 4H); b: 2.67 (t, *J* = 4.5, 4H); d: 6.60 (s, 2H), 6.16 (s, 2H)	a: 30.68; b: 34.61; c: 169.27
5f	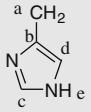	a: 3.34 (d, *J* = 7.0, 4H); c: 9.13 (s, 2H); d: 7.59 (s, 2H); e: 14.9 (s, 1H), 14.6 (s, 1H)	a: 34.59; b: 126.95; c: 134.56; d: 118.73
5g	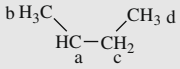	a: 1.99 (m, 2H); b: 0.95 (d, *J* = 4.0, 6H); c: 1.48 (m, 4H); d: 0.91 (t, *J* = 6.5, 6H)	a: 36.26; b: 14.33; c: 25.71; d: 12.01
5h	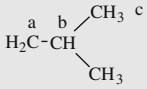	a: 1.54 (m, 4H); b: 1.88 (m, 2H); c: 0.98 (d, *J* = 4.0, 12H)	a: 25.44; b: 44.86; c: 22.71
5i	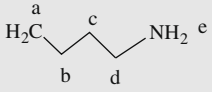	a: 2.84 (m, *J* = 6.0, 4H); b: 1.63 (m, 4H); c: 1.88 (m, *J* = 7.0, 4H); d: 3.75 (m, *J* = 4.0, 4H); e: 8.25 (s, 4H)	a: 34.61; b: 21.75; c: 29.63; d: 38.67
5j	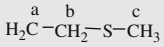	a: 1.97 (q, *J* = 7.5, 4H); b: 2.56 (t, *J* = 5.5, 4H); c: 2.11 (s, 6H)	a: 34.71; b: 30.07; c: 18.15
5k	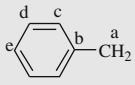	a: 3.19 (dd, *J* = 10.5, *J* = 4.5, 4H); c: 7.30 (d, *J* = 4.5, 4H), d: 7.16 (d, *J* = 4.0, 4H); e: 7.27 (t, *J* = 8.5, 2H);	a: 36.22; b: 135.24; c: 127.73; d: 129.08; e: 129.95
5l		b: 1.99 (m, *J* = 6.0, 4H); c: 1.90 (m, *J* = 6.0, 4H); d: 3.26 (m, *J* = 6.0, 4H)	b: 33.67; c: 25.24; d: 46.74
5m		a: 4.11 (d, *J* = 6.0, 4H); b: 4.52 (s, 2H)	a: 64.37
5n	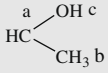	a: 4.34 (m, 2H); b: 1.33 (d, *J* = 5.5, 6H); c: 4.58 (s, 2H)	a: 71.59; b: 20.39
5o	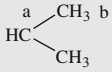	a: 2.18 (m, *J* = 6.0, 2H); b: 2.12 (d, *J* = 7.5, 12H)	a: 29.78; b: 18.97
5p	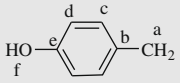	a: 3.20 (dd, *J* = 8.0, *J* = 5.0, 4H); c: 7.14 (d, *J* = 8.0, 4H); d: 7.12 (d, *J* = 8.0, 4H); f: 10.17 (s, 2H)	a: 37.52; b: 133.63; c: 130.27; d: 121.45; e: 150.18
5q	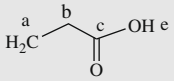	a: 2.24 (m, *J* = 7.0, 4H); b: 2.51 (t, *J* = 9.5, 4H); e: 12.34 (s, 2H)	a: 27.80; b: 31.30; c: 177.31
5r	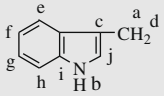	a: 3.34 (dd, *J* = 12.0, *J* = 4.0, 4H); b: 10.94 (s, 2H); e: 7.42 (d, *J* = 2.5, 2H), g: 7.26 (d, *J* = 10.5, 2H), f and h: 7.17 (m, *J* = 4.5, 4H); j: 6.82 (d, *J* = 7.5, 2H)	a: 26.20; c: 106.19; d: 126.65; e: 118.11; f: 119.61; g: 122.31; h: 112.24; i: 136.41; j: 125.34

[a] Compound **5e** has no R.

Table 12
^{13}C NMR data of **5a–r** except R

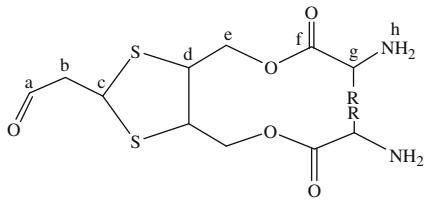

	Ca	Cb	Cc	Cd	Ce	Cf	Cg
5a	203.96	57.49	44.66	48.81	66.03	170.20	50.74
5b	204.28	54.16	43.17	48.64	65.78	172.31	52.45
5c	203.15	53.75	44.71	49.13	65.38	171.13	50.30
5d	203.41	55.41	45.57	50.50	64.63	173.68	53.78
5e	204.39	56.47	44.21	49.03	65.35	167.63	44.21
5f	203.21	56.46	44.74	51.50	65.01	168.16	54.09
5g	204.15	56.50	44.75	49.83	64.37	168.76	53.93
5h	203.79	56.44	44.86	50.03	64.76	169.15	50.82
5i	203.85	56.46	45.36	50.59	64.93	169.43	52.16
5j	203.19	56.33	44.39	50.35	64.71	168.89	52.69
5k	204.01	56.69	45.02	50.54	64.55	168.87	53.60
5l	204.18	59.73	44.36	50.46	65.25	169.34	56.39
5m	203.48	56.44	44.51	50.32	65.74	168.93	56.19
5n	203.89	59.44	44.45	50.72	65.31	166.92	56.68
5o	203.44	57.82	45.81	50.55	65.38	168.85	56.06
5p	203.17	56.96	45.88	50.53	65.38	169.38	54.72
5q	203.51	56.47	40.93	50.55	65.82	172.46	53.98
5r	204.17	64.73	43.59	50.32	65.58	169.55	56.29

transplanted once per week. Subcutaneous tumors were implanted by injecting 0.2 mL of NS containing 4×10^7 viable tumor cells under the skin on the right oxter. Twenty-four hours after implantation, the tumor-bearing mice were randomized into 20 experimental groups (10 per group). All mice were given a daily ip injection of cytarabine (positive control, 89.28 μmol/kg/day in 0.2 ml of NS), or NS (negative control, 0.2 ml), or **5a–r** (44.64 μmol/kg/day in 0.2 ml of NS) for seven consecutive days. Twenty-four hours after the last administration, all mice were sacrificed by diethyl ether anesthesia, and the tumors were dissected and weighed. The inhibitory rate of tumor growth was calculated using the equation: Inhibition = (tumor weight from negative control mice) − (tumor weight from **5a–r** or cytarabine treated mice) ÷ (tumor weight from negative control mice).

4.4. UV and CD spectral studies on 5a–r

UV–vis spectra of **5a–r** (pH 3.5–4.0, aqueous solution, 0.1 mM, 25 °C) were recorded with a Shimadzu 2550UV–visible spectrophotometer over the range of 200–800 nm. Circular dichroism (CD) spectra of **5a–r** (pH 3.5–4.0, aqueous solution, 1 mM, 25 °C) were obtained on a JASCO J-810 spectropolarimeter with JASCO Canvas Program (Model J-810, Jasco, Japan) over the range of 200–750 nm.

Acknowledgements

This work was finished in Beijing Area Major Laboratory of Peptide and Small Molecular Drugs; supported by PHR (IHLB, KZ200810025010) and Special Project (2008ZX09401-002) of China.

References and notes

1. Momekov, G.; Bakalova, A.; Karavanova, M. *Curr. Med. Chem.* **2005**, *12*, 2177.
2. Hurley, L. H. *Nat. Rev. Cancer* **2002**, *2*, 188.
3. Martinez, R.; Chacon-Garcia, L. *Curr. Med. Chem.* **2005**, *12*, 127.
4. Meester, C. *Mutat. Res.* **1995**, *339*, 139.
5. Funayama, Y.; Nishio, K.; Wakabayashi, K.; Nagao, M.; Shimoi, K.; Ohira, T.; Hasegawa, S.; Saijo, N. *Mutat. Res. Lett.* **1999**, *9*, 3319.
6. AUTHOR: PLEASE PROVIDE MORE DETAILS.
7. Al-Allaf, T. A. K.; Rashan, L. J. *Eur. J. Med. Chem.* **1998**, *33*, 817.
8. Cao, R.; Peng, W.; Chen, H.; Ma, Y.; Liu, X.; Hou, X.; Guan, H.; Xu, A. *Biochem. Biophys. Res. Commun.* **2005**, *338*, 1557.
9. Li, N.; Yang, X. *Biochem. Biophys. Res. Commun.* **2005**, *331*, 947.
10. Vijayalakshmi, R.; Kanthimathi, M.; Subramanian, V.; Nair1, B. U. *Biochem. Biophys. Res. Commun.* **2000**, *271*, 731.
11. Thulstrup, P. W.; Thormann, T.; Spanget-Larsen, J.; Bisgaard, H. C. *Biochem. Biophys. Res. Commun.* **1999**, *265*, 416.
12. Jiang, X.; Shang, L.; Wang, Z.; Dong, S. *Biophys. Chem.* **2005**, *118*, 42.
13. Desoize, B.; Madoulet, C. *Crit. Rev. Oncol. Hematol.* **2002**, *42*, 317.
14. Zorbas-Seifried, S.; Jakupec, M. A.; Kukushkin, N. V.; Groessl, M.; Hartinger, C. G.; Semenova, O.; Zorbas, H.; Kukushkin, H. V. Y.; Keppler, B. K. *Mol. Pharmacol.* **2007**, *71*, 357.
15. Dai, J.; Punchihewa, C.; Mistry, P.; Ooi, A. T.; Yang, D. *J. Biol. Chem.* **2004**, *279*, 46096.
16. Yang, F.; Chen, Y.; Duan, W.; Zhang, C.; Zhu, H.; Ding, J. *Int. J. Cancer* **2006**, *119*, 1184.
17. Rodrıguez, D.; Quiros, L. M.; Salas, J. A. *J. Biol. Chem.* **2004**, *279*, 8149.
18. Chianga, L.; Ng, L. T.; Linc, I. C.; Kuo, P.; Lin, C. *Cancer Lett.* **2006**, *237*, 207.
19. Hansch, C.; Leo, A.; Schmidt, C.; Jow, P. Y. C. *J. Med. Chem.* **1980**, *23*, 1095.
20. Montgomery, J. A.; McCaleb, G. S.; Johnston, T. P.; Mayo, J. G.; Laster, W. R., Jr. *J. Med. Chem.* **1977**, *20*, 291.
21. Johnston, T. P.; McCaleb, G. S.; Clayton, S. D.; Frye, J. L.; Krauth, C. A.; Montgomery, J. A. *J. Med. Chem.* **1977**, *20*, 279.
22. Janovec, L.; Sabolova, D.; Kozurkova, M.; Paulikova, H.; Kristian, P.; Ungvarsky, J.; Moravcikova, E.; Bajdichova, M.; Podhradsky, D.; Imrich, J. *Bioconjugate Chem.* **2007**, *18*, 93.
23. Kawakami, M.; Koya, K.; Ukai, T.; Tatsuta, N.; Ikegawa, A.; Ogawa, K.; Shishido, T.; Chen, L. B. *J. Med. Chem.* **1997**, *40*, 3151.
24. Sanyal, U.; Nanda, R.; Samanta, S.; Pain, A.; Dutta, S.; Verma, A. S.; Rider, B. J.; Agrawal, K. C. *Cancer Lett.* **2000**, *155*, 89.
25. Chang, H.; Yamato, O.; Yamasaki, M.; Ko, M.; Maede, Y. *Cancer Lett.* **2005**, *223*, 47.
26. Bi, L.; Zhao, M.; Wang, C.; Peng, S.; Winterfeldt, E. *Eur. J. Org. Chem.* **2000**, 2669.
27. Bi, L.; Zhang, Y.; Zhao, M.; Wang, C.; Chan, P.; Tok, J. B.-H.; Peng, S. *Bioorg. Med. Chem.* **2005**, *13*, 5640.
28. Chauhan, M.; Arjmand, F. *J. Organomet. Chem.* **2007**, *692*, 5156.
29. Kumar, R. S.; Arunachalam, S. *Polyhedron* **2007**, *26*, 3255.
30. Shaikh, A. R.; Ismael, M.; Carpio, C. A. D.; Tsuboi, H.; Koyama, M.; Endou, A.; Kubo, M.; Broclawikc, E.; Miyamoto, A. *Bioorg. Med. Chem. Lett.* **2006**, *16*, 5917.
31. Doddareddy, M. R.; Cho, Y. S.; Koh, H. Y.; Pae, A. N. *Bioorg. Med. Chem.* **2004**, *12*, 3977.